

Modelling the response of UHPFRC panels to explosive loading

G. K. Schleyer¹, S. J. Barnett¹, S. G. Millard¹ & G. Wight²

¹*School of Engineering, University of Liverpool, UK*

²*VSL Australia Pty Ltd, Melbourne, Australia*

Abstract

Explosive testing of full-size fibre-reinforced concrete panels was conducted at GL Industrial Services at Spadeadam test site, Cumbria, England in 2008. The panels were manufactured by VSL Australia and shipped to Spadeadam for testing. This paper reports these tests and a simplified analysis of the response of the panels. Each panel measured 3.5m by 1.3m by 100mm thick. The panels were contained within a large concrete enclosure to minimise clearing around the sides from the blast wave and placed between 7m and 12m from a 100 kg TNT equivalent explosive charge. Two of the panels were fabricated with different levels of steel fibre dosage. The remaining two panels were fabricated with steel fibres together with supplementary steel bar reinforcement. Numerical computer modelling was carried out using the Autodyn package to predict the behaviour of the four panels before testing. Based on the predictive modelling, each panel was placed a suitable distance from the explosive charge so as to cause permanent damage but not total structural collapse. The maximum flexural tensile strain rate evaluated on the back face of the panel was in the region of 1.0s^{-1} . Simplified modelling of the panels was also carried out using a single-degree-of-freedom representation together with a resistance-deflection relationship that took account of characteristic brittle cracking and ductile softening behaviour following ultimate capacity. An outline of the method with results is given in the paper.

Keywords: fibre-reinforced concrete, explosive testing, SDOF modelling, ductile softening behaviour.



1 Introduction

Ultra high performance fibre-reinforced concrete (UHPFRC) has been recently developed (Richard and Cheyrezy [1]) and has material properties which are much improved from those of conventional concrete. UHPFRC contains a very high cement content and very low water-cement ratio (typically 0.15-0.18), which is achieved using a super-plasticiser. In addition, the only aggregate used is fine silica sand, together with a high dosage of fine high tensile steel fibres of the order of 0.2 mm in diameter. Elevated temperature curing at 90 °C enables early-age compressive cube strength of between 150-200 MPa to be achieved. In addition, a flexural tensile strength in the range of 25-50 MPa is provided by the inclusion of the steel fibres. UHPFRC also has a high fracture energy of around 20,000-40,000 J/m².

These properties suggest that UHPFRC could be a suitable material to resist blast and impact loading. Studies were carried out in the UK and Australia, (Rebentrost and Wight [2]) to investigate the properties of UHPFRC under impact and explosive loading. Preliminary results from the UK study were presented at PROTECT 2007 (Barnett et al. [3]) and showed that under quasi-static loading a high flexural tensile strength could be achieved which was sensitive to the dosage of steel fibres in a non-proportionate manner. Further results of the sensitivity of UHPFRC material properties to the strain rate applied during high-speed loading were reported at PROTECT 2009 (Millard et al. [4]) and focus primarily on the flexural tensile and shear strengths. Back face tensile spalling and shear punching are thought to be two critical modes of failure for conventional concrete under blast or high-speed impact loading (Magnusson and Hallgren [5]).

A collaborative research programme between the University of Liverpool and the University of Sheffield has made use of drop hammer and Hopkinson bar test facilities to investigate the dynamic increase factor (DIF) of UHPFRC in both flexural and shear behaviour. The results are described by Millard et al. [6] along with an independent study of the same. The results from both studies correlate well and reveal that a DIF of the flexural tensile strength rising from 1.0 at 1.0s⁻¹ on a slope of 1/3 on a log (strain rate) versus log (DIF) graph can be used for design purposes. The results also show that no significant increase in shear strength is to be gained at high loading rates. Results have been reported for conventional concrete at high strain rates in several publications [7-9].

The collaborative programme culminated in a series of small-scale and large-scale explosive tests using the University Sheffield's field test site at Buxton and the facilities at RAF Spadeadam test site. The results suggest that UHPFRC is suitable for blast and impact mitigation applications particularly in counteracting the threat of an urban terrorist attack. This paper focuses on the full-scale tests at RAF Spadeadam and simplified modelling using single-degree-of-freedom (SDOF) procedures.



2 Full-scale tests

Explosive testing of full-size panels was conducted at RAF Spadeadam, Cumbria. Four panels were manufactured by VSL Australia Pty Ltd, Melbourne and transported to Spadeadam for testing. Each panel measured approx. 3.5m by 1.3m by 100mm thick. The panel was positioned vertically and supported along the upper and lower edges so that it spanned one-way. Each panel was contained within a large concrete enclosure with steel side plates to minimise clearing. The enclosure prevented the blast pressure wave from reaching the back face of the panel and reducing the loading on the front face. A 100kg TNT equivalent explosive charge was used to load the panels with stand-offs between 7m and 12m.

Numerical computer modelling was also carried out using the Autodyn package to predict the behaviour of the four panels prior to testing. Some of the panels were instrumented with a contactless laser displacement transducer to measure the mid-span displacement during blast loading. In addition a simple mechanical friction “broomstick gauge” was used to measure the maximum displacement. The maximum flexural tensile strain rate evaluated on the back face of the panel during full-scale blast loading was estimated to be in the region of $1.0s^{-1}$.

2.1 VSL panels

Two of the full-size panels were fabricated with different levels of steel fibre dosage, 2% and 4% by volume, respectively. The fibre lengths were 13 mm and 25 mm by 0.2 mm in diameter. The remaining two panels were fabricated with steel fibres together with identical additional steel bar reinforcement. Based on predictive modelling, each panel was placed at a stand-off from the explosive charge designed to cause permanent damage but not structural collapse as given in table 1.

Table 1: Stand-off distances and fibre content by volume of test panels.

Panel #	Fibres	Additional steel bar reinforcement?	Stand-off (m)
1	2% 13mm long	Yes	9
2	2% 13mm long	No	12
3	2% 13mm + 2% 25mm	No	12
4	2% 13mm long	Yes	7

VSL carried out a static analysis of the test panels and produced moment-curvature relationships as shown in fig. 1. This data is also summarised in table 2 and was used to develop a resistance-deflection function for the SDOF modelling described in section 3. The stiffness given in table 2 is based on a



Table 2: Summary of static analysis of test panels.

Panel #	M_{\max} (kNm)	Curvature at M_{\max} ($\text{mm}^{-1} \times 10^{-5}$)	Deflection at M_{\max} (mm)	Stiffness k (kPa/mm)	R_{\max} (kPa)
1	194.5	8.582	39.4	2.48	97.7
2	123.8	7.161	27.4	2.27	62.2
3	154.3	7.637	31.2	2.48	77.5
4	194.5	8.582	39.4	2.48	97.7

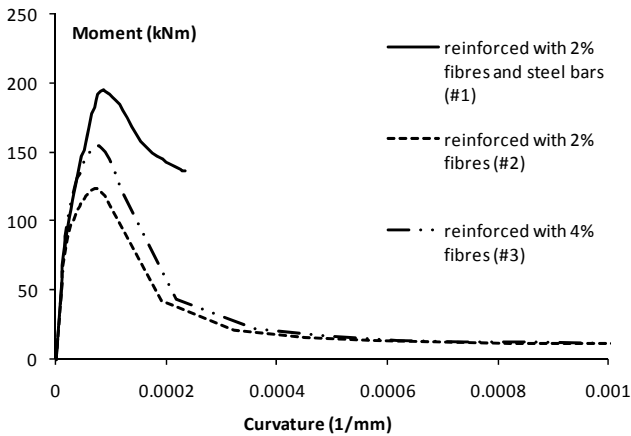


Figure 1: Moment-curvature relationship of VSL panels.

linear approximation to maximum capacity (deflection at M_{\max}). The initial stiffness is higher.

2.2 Test results

The test panels were arranged in ‘arena’ style layout in which a number of targets are positioned at various stand-offs around a central explosive charge. The blast wave produced by detonating the explosive charge radiates in all directions and so can be used to load a certain number of test pieces at the same time according to their stand-off distance from the charge. The panels were all set up to receive the air blast loading with a normal angle of incidence to the propagating blast wave. The panels would therefore experience a reflected pressure and impulse. The loading can be readily estimated using air-blast data from TM 5-1300 [10].

The results of the tests are summarised in table 3. Fig. 2 shows the two unreinforced panels #2 and #3 after testing permanently deformed by 180mm and 90mm, respectively with no apparent elastic rebound.

Table 3: Test results.

Panel #	Stand-off (m)	Maximum deflection (mm)	Permanent deflection (mm)
1	9	110	20
2	12	180	180
3	12	90	90
4	7	210	50

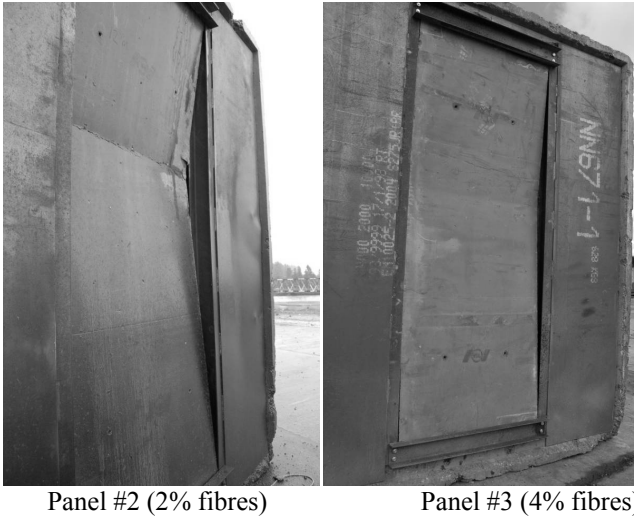


Figure 2: Unreinforced panels #2 and #3 after testing at 12m stand-off.

3 SDOF modelling

SDOF methods are based on the representation of the actual structure by an equivalent spring-mass system that is constrained to have only one degree of freedom. The equivalent system parameters, mass, spring stiffness, spring yield load and applied force (M_e , k_e , R_{me} and F_e respectively) are selected such that the deflection of the equivalent concentrated mass, M_e , is the same as that for some significant point on the structure, usually the point of maximum deflection as shown in fig. 3. Forces and stresses are not directly equivalent. The constants of the spring-mass system are evaluated on the basis of an assumed deformed shape of the structure, normally the approximate shape as that resulting from the static application of the loading.

The load transformation factor, K_L , which relates the equivalent force on the spring-mass system to the total force on the actual structure, is evaluated from a consideration of the work done by the equivalent spring-mass system and the structural model. Similarly, the mass transformation factor, K_M , which relates the lumped mass on the spring-mass system to the total mass of the actual structure, is evaluated from a consideration of the kinetic energy of the equivalent spring-mass system and the structural model.

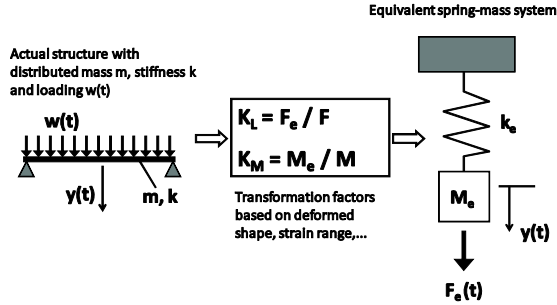


Figure 3: SDOF representation.

The load transformation factor, $K_L = F_e / F = k_e / k$ where k and F are the linear spring stiffness and total force for the actual structure respectively and k_e and F_e are the spring stiffness and equivalent force for the spring-mass system. The mass transformation factor $K_M = M_e / M$ where M is the total mass for the actual structure and M_e is the lumped mass for the spring-mass system.

SDOF analysis can be used for any duration of load and can be used for both elastic and elastic-plastic behaviour. The SDOF system is therefore a good model of the dynamics of the real system and allows non-linear behaviour to be modelled. Further details of the method and calculation of the equivalent spring-mass properties can be found in Biggs [11] and Baker et al. [12].

A structural member's capacity to resist a load (static or dynamic) can be defined by a resistance function which combines elastic stiffness with plastic energy absorption. Standard SDOF methods are based on an effective bi-linear resistance function as shown in fig. 4 for a beam with fixed ends and simple

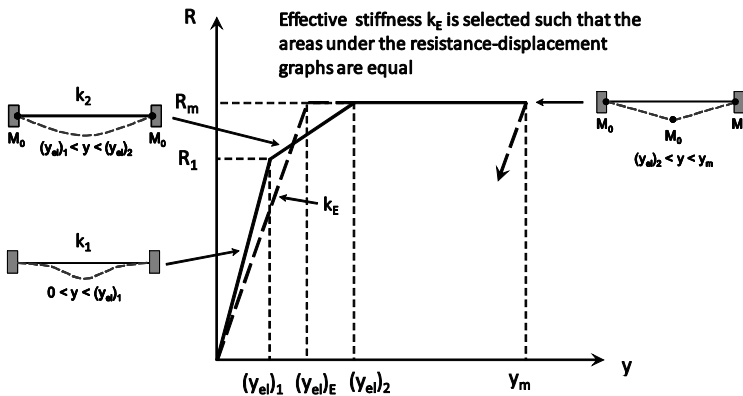


Figure 4: Effective bi-linear resistance-deflection relationship for a beam with fixed supports as used in the SDOF method.

elastic-perfectly plastic material behaviour. This representation is usually adequate in the context of rapid design screening for modelling the flexural behaviour of ductile steel beams and RC beams and slabs.

However, the FRC panels exhibit characteristic softening behaviour due to a combination of brittle cracking and ductile yielding after reaching their ultimate capacity. Standard graphical or numerical implementation of the SDOF method do not provide for definition of softening or hardening behaviour after yielding. Enhanced numerical implementation of SDOF methods have been developed to allow typical hardening or softening behaviour or a combination of both to be modelled in the analysis. More accurate definition of the resistance-deflection relationship leads to better predictions of structural response. SBEDS [13] is an engineering spreadsheet tool intended for use by structural engineers with knowledge of structural dynamics and blast effects. It is a product of the US Army Corps of Engineers (USACE) developed by several consulting engineering companies in the US contracted by the USACE protective Design Centre (PDC). It enables the user to define a resistance-deflection function with up to 5 points, shown typically in fig. 5. This tool was used for the SDOF analysis of the test panels.

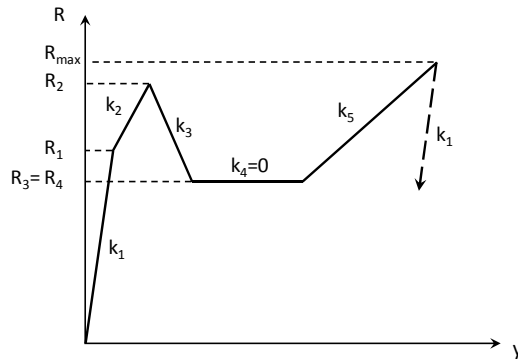


Figure 5: Typical resistance-deflection function as used in SBEDS [13].

3.1 SDOF parameters

The parameters for the SDOF analysis were determined from the static mechanical properties and moment-curvature relationships supplied by VSL, shown in fig. 1 and summarised in tables 4 and 5. A dynamic increase factor (DIF) of 1.2 and 5% critical damping was applied to panels #1 and #4 with additional steel bar reinforcement. This effectively raised the maximum resistance e.g. in panel #1 from 97.7 to 117.2 kPa. Subsequent points were simply raised by the same amount. A DIF=1.1 and no damping was applied to panels #2 and #3, reinforced only with steel fibres.

Table 4: SDOF model parameters.

Parameter	Value	Units
Length, L	3.5	m
Load-mass factor (elastic)	0.78	-
Load-mass factor (plastic)	0.66	-
Area, A	4.55	m ²
Density, ρ	2450	kg/m ³
Mass, M	1115	kg

Table 5: Resistance-deflection parameters.

Panel #	1	2	3	4	Units
k ₁	46.9	2.27	2.48	46.9	kPa/mm
R ₁	29.1	68.42	85.25	29.1	kPa
k ₂	1.79	-1.0	-1.0	1.79	kPa/mm
R ₂	117.2	20.0	20.0	117.2	kPa
k ₃	-0.18	-0.1	-0.1	-0.18	kPa/mm
R ₃	95.64	10.0	10.0	95.64	kPa
k ₄	-0.05	-0.01	-0.01	-0.05	kPa/mm
R ₄	87.74	5.02	5.02	87.74	kPa
k ₅	0.0	0.0	0.0	0.0	kPa/mm
R ₅	87.74	5.02	5.02	87.74	kPa

The load parameters given in table 6 were determined using the data from TM 5-1300 [10] based on cube root scaling of TNT equivalent surface bursts. The free field parameters of reflected pressure and impulse are well defined at a distant target. The equivalent load duration assumes a right-angled triangular load pulse shape for the blast load. Only the positive phase of the loading was considered in the analysis; the negative phase was ignored.

Table 6: Load parameters.

Stand-off (m)	Peak reflected pressure (kPa)	Peak reflected impulse (kPa-msec)	Equivalent load duration (msec)
7	2488	2400	1.9
9	1160	1754	3.0
12	498	1240	5.0

3.2 SDOF results

The analysis results along with the test results for comparison are summarised in table 7. The deflection vs. time graphs for each of the 4 panels are shown in figs 6–9 together with their respective resistance (kPa) vs. deflection (mm) graph. These results are discussed in section 4.



Table 7: Comparison of results.

Panel #	Maximum deflection (mm)		Permanent deflection (mm)	
	Test	SDOF	Test	SDOF
1	110	106	20	46
2	180	179	180	175
3	90	90	90	78
4	210	200	50	147

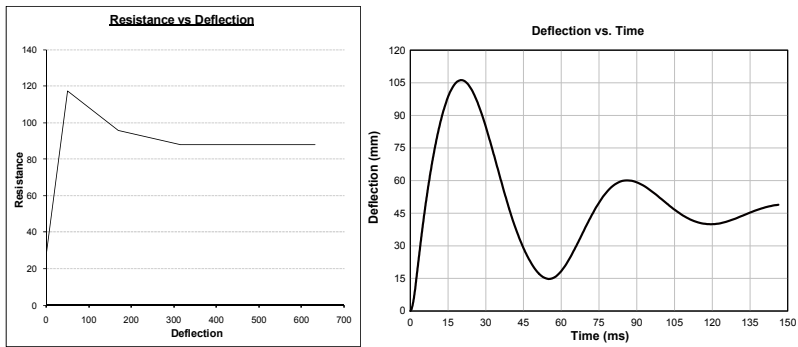


Figure 6: Panel #1 SDOF model input resistance-deflection and output deflection-time graphs.

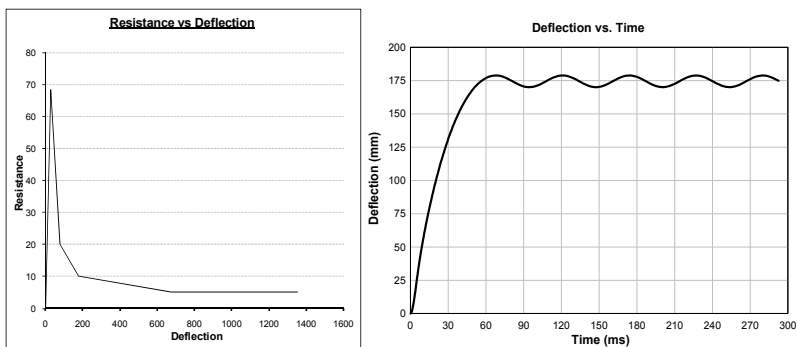


Figure 7: Panel #2 SDOF model input resistance-deflection and output deflection-time graphs.

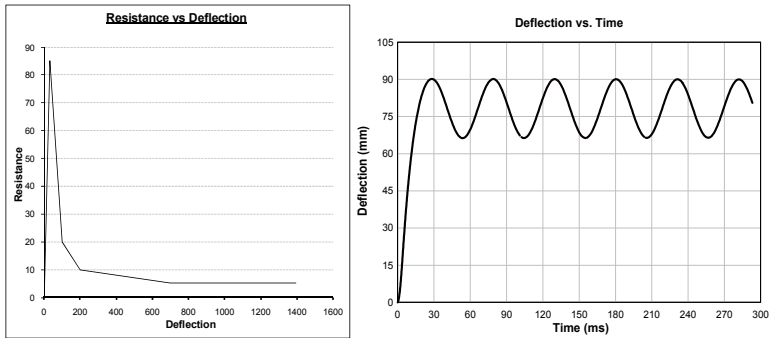


Figure 8: Panel #3 SDOF model input resistance-deflection and output deflection-time graphs.

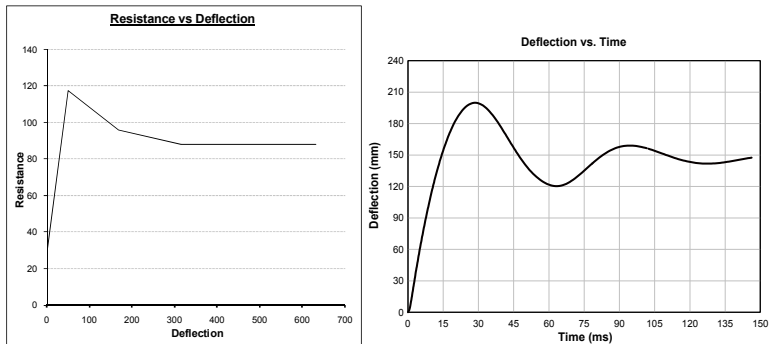


Figure 9: Panel #4 SDOF model input resistance-deflection and output deflection-time graphs.

4 Discussion

It is clear that the panels #1 and #4 containing both steel fibre and additional steel bar reinforcement have significant spring-back which is partially captured by the SDOF model but not to the extent exhibited in the tests. In fact the recording of test panel #1 showed a rebound deflection of the order of 75 mm outwards. However, the peak deflections modelled in the SDOF procedure for panels #1 and #4 correlate much better with the test results than the permanent deflections. Test panels #2 and #3, which contained only steel fibre reinforcement, exhibited characteristic brittle behaviour following cracking and yielding. It would appear that this softening behaviour was captured by the SDOF procedure since the permanent deflections correlate reasonably well. It is interesting to note that the SDOF method predicts a small elastic rebound. It is also noted that the SDOF procedure even with its limitations is capable of

bounding the problem. The uplift in strength introduced into the modelling was considered appropriate at this rate of loading. The influence of the additional steel bar reinforcement is clearly significant, the extent of which may only be realised in a detailed finite element modelling procedure. The yield line failure at or near the mid-span of the panel together with no rear face spalling due to the embedded steel fibres was entirely consistent with this type of structure.

5 Conclusions

Four UHPFRC full-size panels were subjected to air blast loading arising from a 100kg TNT equivalent explosive charge. Two of the panels contained both steel bar and steel fibre reinforcement while the other panels contained only steel fibre reinforcement. One panel contained 4% steel fibres by volume while the remaining panels contained 2% steel fibres by volume. Blast loading caused various degrees of permanent damage in the form of a yield line at or near the mid-span but not total structural collapse, by virtue of the stand-off distance from the charge. A consistent approach to modelling the four test panels as a one-way spanning member using an SDOF procedure gave reasonably good correlation and demonstrated the versatility of the SDOF method. A particular feature of the SDOF procedure that contributed to a successful result was the definition of the resistance-deflection relationship to include softening behaviour. The simplified procedure was unable, however, to entirely capture the significant elastic rebound exhibited in the panels with additional steel bar reinforcement. Further investigation is necessary.

Acknowledgements

This study has been carried out with support from the Engineering and Physical Sciences Research Council (EPSRC), under the “Think Crime-4” managed programme. The investigators are grateful for the support of the following industrial collaborators: Centre for the Protection of National Infrastructure (CPNI), Bekeart Ltd, Elkem Ltd, VSL (Australia), Fosroc Ltd, Castle Cement, and the Appleby Group.

References

- [1] Richard, P. & Cheyrezy, M., Composition of reactive powder concretes. *Cement Concrete Research*, **25(7)**, pp. 1501-1511, 1995.
- [2] Rebertrost, M. & Wight, G., Behaviour and resistance of ultra high performance concrete to blast effects. *Proc. of 2nd Int. Symposium on Ultra High Performance Concrete*, eds. E. Fehling, M. Schmidt, and S. Stürwald, pp. 735-742, 2008.
- [3] Barnett, S.J., Millard, S.G., Soutsos, M.N., Schleyer, G.K., & Tyas, A., Flexural Performance of UHPFRC. *Proc. of PROTECT 2007: Structures under Extreme Loading*, 2007.



- [4] Millard, S.G., Barnett, S.J., Schleyer, G.K., Tyas, A. & Rebentrost, M., Explosion and Impact Resistance of Ultra High Performance Fibre Reinforced Concrete. *Proc. of PROTECT 2009: Structures under Extreme Loading*, 2009.
- [5] Magnusson, J., & Hallgren, M., Reinforced high strength concrete beams subjected to air blast loading. *Proc. of 8th Conf. on Structures under Shock and Impact*, eds. N. Jones & C.A. Brebbia, WIT, pp. 53-62, 2004.
- [6] Millard, S.G., Molyneaux, T.C., Barnett, S.J. & Gaob, X., Dynamic enhancement of blast-resistant concrete under flexural and shear loading. Submitted to *Int. Journal of Impact Engineering*, 2010.
- [7] Malvar, L.J. & Ross, C.A., Review of strain rate effects for concrete in tension. *ACI Materials Journal*, **95(6)**, pp. 735-739, 1998.
- [8] Solomos, G. & Berra, M., Compressive behaviour of high performance concrete at dynamic strain-rates. *Proc. of 6th RILEM Symposium on Fibre-Reinforced Concretes*, eds. M. Di Prisco, R. Felicetti & G.A. Plizzari, RILEM Publications S.A.R.L., pp. 421-430, 2004.
- [9] Ulfkjaer, J., Labibes, K., Solomos, G. & Albertini, C., Tensile failure of normal concrete and steel fibre reinforced concrete at high strain rates. *Proc. of 3rd Fracture Mechanics of Concrete Structures*, pp. 585-592, 1998.
- [10] TM 5-1300, Structures to resist the effects of accidental explosions, 1990, <http://www.ddesb.pentagon.mil/tm51300.htm>.
- [11] Biggs, J.M., *Introduction to Structural Dynamics*, McGraw Hill, 1964.
- [12] Baker, W.E., Cox, P.A., Westine, P.S., Kulesz, J.J. & Strehlow, R.A., *Explosion Hazards and Evaluation*, Elsevier, 1983.
- [13] SBEDS v.4.1, Protective Design Centre, U.S. Corps of Engineers, 2009, <https://pdc.usace.army.mil/software/sbeds/>.

